a favored interface between the β-Sn and the (110) planes in the Si matrix. The excellent lattice match between the (100) planes of the β-Sn and the (110) Si is clearly the driving force for this elongation, leading to an extended coherent interface. Symmetry allows an equivalent elongation in the perpendicular in-plane $<110>_{Si}$ direction (Fig. 1D).

High-resolution Z-contrast tomography in the STEM was used to elucidate the formation mechanism of embedded quantum dots. We have identified embedded quantum dots with both the α-Sn and β-Sn phases, with a transformation into β-Sn beyond a critical diameter of ~8 nm. Some quantum dots are formed outside the embedded layers due to diffusion of Sn from the layers to fill Si voids. These dots are formed by Stranski-Krastonov growth, filling from one side of the void to the other after an initial wetting of the surface of ~1 to 2 monolayers. These results demonstrate that STEM tomography can directly determine the location, size, shape, structure, and formation mechanism of embedded nanostructures in 3D with a resolution of 1 nm^3, which is essential information for all of the nanosciences.

References and Notes

1. X. Michalet *et al.*, *Science* **307**, 538 (2005).
2. Y. Lin *et al.*, *Nature* **434**, 55 (2005).
3. A. P. Alivisatos, *J. Phys. Chem.* **100**, 13266 (1996).
4. T. Mokari, E. Rothenberg, I. Popov, R. Costi, U. Banin, *Science* **304**, 1787 (2004).
5. J. Su *et al.*, *Appl. Phys. Lett.* **86**, 013105 (2005).
6. J. M. Cowley, *Principles and Techniques of Electron Microscopy; Biological Applications* (Van Nostrand Reinhold, New York, 1976), vol. 6.
7. S. B. Chikkannanavar, D. E. Luzzi, S. Paulson, A. T. Jonson Jr., *Nano Lett.* **5**, 151 (2005).
8. N. D. Browning, M. F. Chisholm, S. J. Pennycook, *Nature* **366**, 143 (1993).
9. S. J. Pennycook, L. A. Boatner, *Nature* **336**, 565 (1988).
10. E. M. James, N. D. Browning, *Ultramicroscopy* **78**, 125 (1999).
11. P. E. Batson, N. Dellby, O. L. Krivanek, *Nature* **418**, 617 (2002).
12. I. Arslan, A. Bleloch, E. A. Stach, N. D. Browning, *Phys. Rev. Lett.* **94**, 025504 (2005).
13. P. A. Midgley, M. Weyland, *Ultramicroscopy* **96**, 413 (2003).
14. L. Goldstein, F. Glas, J. Y. Marzin, M. N. Charasse, G. Le Roux, *Appl. Phys. Lett.* **47**, 1099 (1985).
15. D. Leonard, M. Krishnamurthy, C. M. Reaves, S. P. DenBaars, P. M. Petroff, *Appl. Phys. Lett.* **63**, 3203 (1993).
16. T. P. Pearsall, Ed., *Quantum Semiconductor Devices and Technologies*, (Kluwer Academic Publishers, Dordrecht, Netherlands, 2000).
17. R. Ragan, K. S. Min, H. A. Atwater, *Mater. Sci. Eng. B* **87**, 204 (2001).
18. Y. Lei *et al.*, *Appl. Phys. Lett.* **82**, 4262 (2003).
19. P. Mock *et al.*, *Proc. SPIE* **4807**, 71 (2002).
20. V. V. Voronkov, R. Falster, *J. Cryst. Growth* **198-199**, 399 (1999).
21. J. Jinschek, U. Kaiser, W. Richter, *J. Electron Microsc.* **50**, 3 (2001).
22. D. J. Eaglesham, A. E. White, L. C. Feldman, N. Moriya, D. C. Jacobson, *Phys. Rev. Lett.* **70**, 1643 (1993).
23. R. W. Vook, *Int. Metals Rev.* **27**, 209 (1982).
24. A. Zangwill, *Physics at Surfaces*, (Cambridge Univ. Press, Cambridge, 1988), pp. 427–432.
25. D. H. Rich, T. Miller, A. Samsavar, H. F. Lin, T.-C. Chiang, *Phys. Rev. B* **37**, 10221 (1988).
26. A. Charrier *et al.*, *J. Phys. Condens. Matter* **13**, L521 (2001).
27. M. Yoshimura, B. An, K. Yokogawa, K. Ueda, *Appl. Phys. A* **66**, S1047 (1998).

28. This work was supported by the Royal Society and the NSF in the form of fellowships for I.A. We thank J. Barnard, the FEI Company, and P. Moeck for helpful discussions and H. Atwater for the samples. The Engineering and Physical Sciences Research Council, the Cambridge Interdisciplinary Research Collaboration in Nanotechnology, the FEI Company, and the Isaac Newton Trust are thanked for financial assistance. This work was supported in part by the U.S. Department of Energy under grant number DE AC05-03ER46057.

Supporting Online Material

www.sciencemag.org/cgi/content/full/309/5744/2195/DC1
Movies S1 to S4

29 June 2005; accepted 2 September 2005
10.1126/science.1116745

Colloidal Jamming at Interfaces: A Route to Fluid-Bicontinuous Gels

K. Stratford,[1] R. Adhikari,[2] I. Pagonabarraga,[2,3] J.-C. Desplat,[1,4] M. E. Cates[2]*

Colloidal particles or nanoparticles, with equal affinity for two fluids, are known to adsorb irreversibly to the fluid-fluid interface. We present large-scale computer simulations of the demixing of a binary solvent containing such particles. The newly formed interface sequesters the colloidal particles; as the interface coarsens, the particles are forced into close contact by interfacial tension. Coarsening is markedly curtailed, and the jammed colloidal layer seemingly enters a glassy state, creating a multiply connected, solidlike film in three dimensions. The resulting gel contains percolating domains of both fluids, with possible uses as, for example, a microreaction medium.

The search for new materials with mesoscale or nanoscale structure is a major theme of current physical science. Routes that exploit spontaneous self-assembly in thermal equilibrium are important (*1*, *2*), but nonequilibrium processes offer more control—because assembly is then governed not just by thermodynamic conditions but by the entire process history [e.g., (*3*–*5*)]. Moreover, the resulting materials may become trapped in deeply metastable states such as colloidal clusters, glasses, and gels (*3*, *5*–*7*), remaining more robust than an equilibrium phase to subsequent changes in thermodynamic conditions. This is a key consideration in determining the shelf-life and flow behavior of everyday products such as paint, vaccines, and yogurt.

We use computer simulations to explore a kinetic pathway that leads to the creation of amorphous soft-solid materials. In such a material, which we call a bicontinuous interfacially jammed emulsion gel (or Bijel) (*8*), a pair of interpenetrating, bicontinuous fluid domains are frozen into a permanent arrangement by a densely jammed monolayer of colloidal particles at the fluid-fluid interface. Such materials may have distinctive properties, stemming directly from the nonequilibrium, arrested nature of the monolayer: Bijels should be highly tunable in elasticity and pore size through the volume fraction ϕ and radius a of the solid particles. (The radius can be varied from micrometers to nanometers without altering the physics of structure formation by the route reported here.) One possible application, explored below, is as a cross-flow microreaction medium in which two immiscible fluids are continuously brought into intimate contact by pumping them in opposite directions through a static Bijel.

To achieve maximal stability of a particle-laden interface, the colloidal particles should be chosen with nearly equal affinity for the two liquids involved (*9*). This creates similar values for the two fluid-solid interfacial tensions, and thus a fluid-fluid-solid contact angle close to 90° (known as neutral wetting). A spherical particle is then in stable equilibrium, with its equator positioned at the fluid-fluid interface. In practice, this equilibrium is so stable that detachment of such a particle cannot be achieved by thermal motion alone (*9*). For neutral wetting, the fluid-solid interfaces have the same total energy regardless of particle position, but the fluid-fluid interfacial area is reduced, by a disk of radius a, when the particle lies midway across the interface. The detachment energy ε is the interfacial energy of this disk, $\varepsilon = \sigma\pi a^2$, with σ the fluid-fluid interfacial tension. Hence $\varepsilon/k_BT = (a/a_0)^2$, where $a_0^2 = k_BT/\pi\sigma$ (k_B is the Boltzmann constant and T is temperature). For $T = 300$ K and σ typically ~0.01 Nm^{-1} or larger, a_0 is 0.4 nm or less. Thus, $\varepsilon/k_BT \geq 10$ even for a particle of 1 nm radius, and

[1]EPCC, [2]SUPA, School of Physics, University of Edinburgh, James Clerk Maxwell Building, Kings Buildings, Edinburgh EH9 3JZ, UK. [3]Departament de Física Fonamental, Universitat de Barcelona, C. Martí i Franqués 1, 08028 Barcelona, Spain. [4]Irish Centre for High-End Computing, Dublin Institute for Advanced Studies, 5 Merrion Square, Dublin 2, Ireland.

*To whom correspondence should be addressed. E-mail: m.e.cates@ed.ac.uk

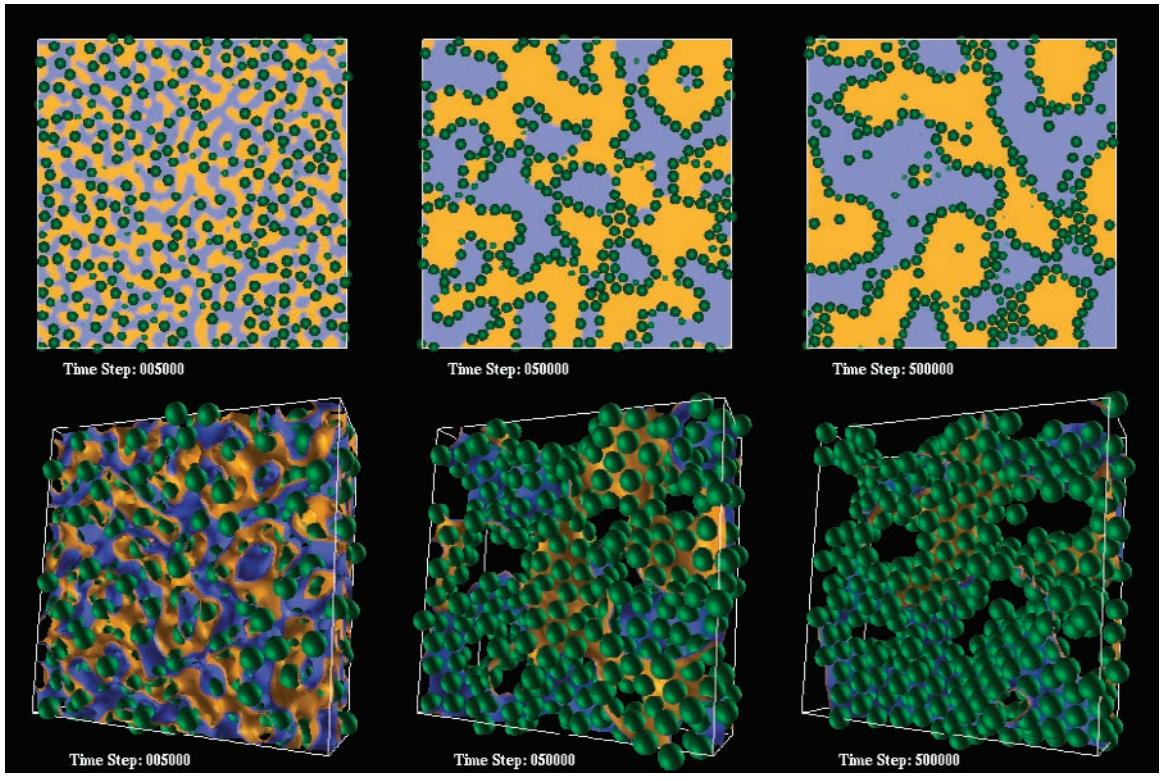

Fig. 1. Time evolution of monodisperse neutrally wetting colloidal particles at volume fraction $\phi = 0.2$ in a binary solvent following a quench. (Upper panels) A 128×128 section through the full simulation (performed on 128^3 lattice) is shown. The two fluids are colored yellow and blue. Monodisperse colloidal particles (green) are shown only if overlapping the plane of the section, with parts lying behind this plane occluded (so that particles whose midpoint is behind the plane appear reduced in size). Sequestration of the particles, followed by near-arrest of the bicontinuous structure, is seen. Frames are at 5000, 50,000, 500,000 LB time steps; for parameter details see (*12*). (Lower panels) A three-dimensional (3D) view of a $64 \times 64 \times 24$ piece cropped from the same simulation with the same time frames. Both fluids are now shown transparent with the two sides of the fluid-fluid interface painted yellow and blue. Sequestration, arrest, and fluid bicontinuity of the resulting structure are all apparent.

thermally activated detachment can be safely neglected for, say, $a \geq 3$ nm.

We consider near-neutral wetting particles suspended in a binary solvent under conditions where the fluids are fully miscible (generally at high temperature) and of roughly equal volume fraction. In the absence of strong attractions between them, the particles will diffuse freely. If the temperature is quenched deep into a two-phase region, the solvents will demix by spinodal decomposition (*10*). A sharp interface between the two fluids develops, and coarsens. During the coarsening, which is driven by the tendency of the interface to reduce its area, the characteristic length scale $L(t)$ initially increases with time in a well-understood manner (*11*), causing bumps on the interface to flatten and necks between neighboring domains of the same fluid to pinch off.

We have studied what happens after this initial separation by simulations (*12*) using the lattice Boltzmann (LB) method (*13*–*17*). We find that, as coarsening proceeds, the interface sweeps through the fluid phases, efficiently collecting and sequestering the colloidal particles. Initially, the attached particles have little effect on the interfacial motion, but as more are collected and the interfacial area shrinks, they soon approach a densely packed monolayer. At this point, the fluid must either (i) stop coarsening at some length scale $L(t) = L^*$ or (ii) thereafter expel particles steadily from the ever-shrinking interface. In our simulations, we see a drastic curtailment of the coarsening and very little particle expulsion. This suggests that the free-energy landscape of the dense colloidal film is such as to trap particles on the interface in a metastable, amorphous state (*18*).

Figure 1 shows the structure as time evolves; for visibility, only a small part [in cross section (upper panels) or crop (lower panels)] of the full system is shown. Movie S1 shows an animation of the observed sequence of events within the cropped region of Fig. 1; this clearly shows the particle sweep-up and the pronounced slow-down of coarsening. Movie S2 shows the entire simulation domain for another run, in which bidisperse particles are used; this prevents development of any local crystalline order in the interfacial colloid layer (arguably visible in Fig. 1). Movie S3 shows a similar subregion for this case as in Movie S1. The results are qualitatively the same; see Fig. 2 for a snapshot at late times. Figure 3 shows the time dependence of the domain size $L(t)$ in each case.

The parameter values chosen for these simulations (*12*) map onto particles of radius $a = 5$ nm in a symmetric pair of fluids each having viscosity $\eta = 10^{-3}$ Pa s and mass density $\rho = 10^3$ kg m^{-3}, with $\sigma = 6 \times 10^{-2}$ N m^{-1} at $T = 300$ K; such values are typical of a short-chain hydrocarbon/water or alcohol/water mixture. Our particles have purely repulsive interactions, with a range extending somewhat beyond their hard-sphere (hydrodynamic) radii (*12*), so that particles remain visibly separated even in a dense monolayer. The parameter mapping is made by matching dimensionless control groups ε/k_BT and $a\rho\sigma/\eta^2$ (*12*, *19*). Brownian motion of the colloidal particles is included (*12*), but has rather little effect during the time regime we can reach by simulation (see below), and would have even less effect with larger particles. We have also checked the role of short-range, thermally reversible bonding among colloids (*7*), but this too has little effect. These observations are attributable to the strong separation between Brownian and interfacial energy scales referred to above.

A number of numerical compromises were made to keep the simulations tractable (*12*). First, the Reynolds number $Re = (dL/dt)\rho a/\eta$ is much larger than in the real system, though we still have $Re \ll 1$ (*19*). Second, the scale separation between the particle radius a and the fluid-fluid interfacial thickness ξ is only modest (a factor of 2 or 3), with the lattice spacing, in turn, not much less than ξ. This gives imperfect discretization of the fluid-fluid interface around particles and may underrepresent the energy barrier to short-scale rearrangements (*12*). Finally, for the physical parameters given above, the effective run-time of our largest simulations is about 300 ns. (For larger particles, say $a = 3$ μm, the equivalent run time would be around 5 ms.)

Although these simulations dramatically confirm our proposed kinetic pathway for creating a fluid-bicontinuous state with a particle-laden interface, they cannot tell us whether this state

is a fully arrested gel on laboratory time scales. Unlike our simulations, the latter vastly exceeds the time scale $\tau = 6\pi\eta a^3/k_BT$ characterizing Brownian motion of colloids. Nonetheless, the observed behavior, particularly for bidisperse particles, is consistent with that of a long-lived, metastable, arrested state. In common with other such states (including colloidal glasses), Bijels might show slow aging behavior as the interface approaches saturation. This may explain the residual late-time dynamics visible in the $L(t)$ curves of Fig. 3. Alongside aging, the slow residual dynamics could be due to the incomplete separation of length scales in LB noted above or, in the monodisperse case, due to a tendency for the interfacial layer slowly to acquire local crystalline order. (Such ordering would not preclude, and might even enhance, eventual structural arrest.) We have also assessed the particle mobility in the interfacial film by measuring the distribution of individual particle displacements at late times. We found this to be dominated by the residual relaxation dynamics of the structure rather than by diffusion within the film.

The near-complete cessation of fluid motion on time scales on the order of τ suggests that further coarsening, which requires expulsion of particles from the interface, cannot take place without colloidal Brownian motion. If, as argued earlier, such motion is ineffective at detaching particles from a static interface, coarsening must cease altogether. In principle, lateral diffusion within a film of fixed area might continue. However, the surface pressure of such a film is estimated (*20*) as $\Pi \sim k_BT/[a^2(\psi_m - \psi)]$, where ψ is the areal fraction and ψ_m that of a maximally close-packed configuration. For this pressure to balance the interfacial tension requires that $\psi_m - \psi \sim (a_0/a)^2$. For large enough particles, this ensures that ψ exceeds any threshold value, so long as this value is less than ψ_m, for the onset of an arrested state within the film.

Further evidence for interfacial arrest was gained by additional, higher-resolution simulations that examine the dynamics of two specific structural motifs characteristic of the bicontinuous structure. One of these is a long cylinder, representing a fluid neck. Without particles the Rayleigh-Plateau instability (*21*) would cause the cylinder to break into droplets. We show in fig. S1 a dense bidisperse colloidal packing on a cylindrical interface. When perturbed, this structure shows no sign of either ordering or breakage, and the initial undulation visibly decays, rather than grows. The structure then arrests, and remains unchanged for the duration of the simulation, which is 10 times as long as the time-to-rupture of an unprotected cylinder. Our second structural motif is a periodically rippled surface, whose bumps are broadly characteristic of a non-necklike section of the bicontinuous interface between fluids. Without particles, the ripple would rapidly be pulled flat by interfacial tension. Figure S2 shows how this process is interrupted by interfacial jamming. After an initial transient decay, the film jams, and bumps on it persist at least 30 times as long as the decay time without particles. There is negligible macroscopic motion during the latter half of this simulation.

These results show that, at sufficient interfacial coverage (*22*), both necks and bumps can arrest by jamming of the adsorbed colloidal layer into a densely packed, and therefore presumably glasslike, state. Because these two structural elements are, in combination, the driving features of bicontinuous coarsening (*21*), their arrest would be enough to prevent coarsening. Hence these studies provide very strong supporting evidence for an eventual arrest of our bicontinuous structure, caused by a jamming transition (*23*) within the colloidal monolayer. This transition is induced by the (capillary) stresses arising from the fluid-fluid tension.

Once the interfacial film has fully arrested, because it percolates in three dimensions, the entire material will acquire solid elasticity at scales beyond L^*. The static modulus G of the resulting gel should scale with the interfacial energy density σ/L; so long as nearly all particles end up on the interface, $L^* \sim a/\phi$ with ϕ the particle volume fraction. For $\sigma = 0.01$ N m^{-1}, $0.01 \le \phi \le 0.1$, and 5 nm $< a <$ 5 μm, we estimate $20 \le G \le 2 \times 10^5$ Pa. This is a very wide "tuning" range for material design. Under nonlinear stress the interfacial area will dilate substantially; only a modest dilation (say 10%) may suffice to cause melting of the particle layer and drastic fluidization. This might instigate both flow and coarsening above some yield stress $Y \cong 0.1\ G$. If the stress falls back below Y, we expect resolidification, possibly with remanent anisotropy (hysteresis). The nonlinear flow behavior of these gels could thus show a remarkable strain-melting, possibly reminsicent of a colloidal glass, but with a much higher stress scale set by interfacial, not Brownian, forces. The estimates above for the material properties of the gel stem from the jamming of colloids by the interfacial forces

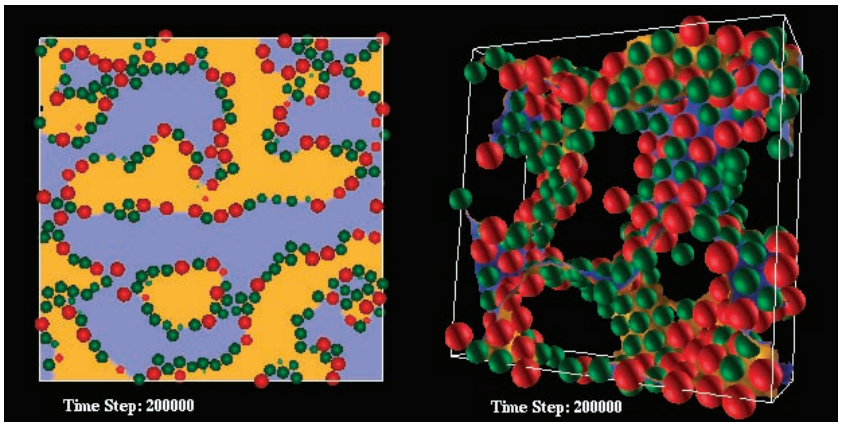

Fig. 2. Structure at 200,000 time steps in a simulation of bidisperse neutrally wetting particles in a binary solvent following a quench, in section and 3D view. Color coding as in Fig. 1 but with larger particles shown in red; size ratio, 1.2:1. **(Left)** A 128 × 128 section; the top left quadrant of this square is coincident with the front face of the 64 × 64 × 24 cuboid used for the 3D view (**right**). There is no sign of local crystalline order in the particle film (visible in Fig. 1, lower panels), although some tendency toward local segregation by particle size is seen. For parameter details see (*12*). The same structure, evolved to 590,000 time steps, is shown in Fig. 4.

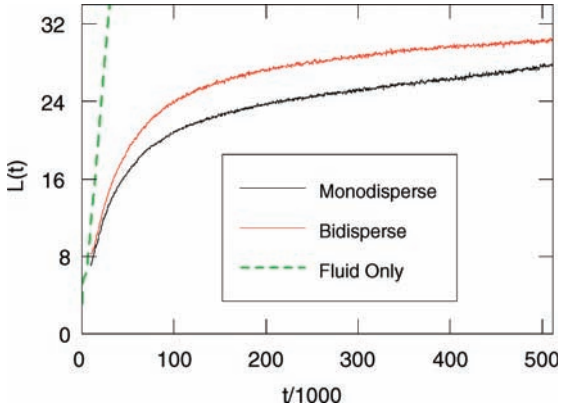

Fig. 3. Time evolution of the structural length scale $L(t)$ for monodisperse (lower curve) and bidisperse (upper curve) particle runs as described in (*12*). L is measured in units of the LB lattice and t in LB time steps. Without particles, coarsening would proceed with the slope indicated by the dotted line (*11*). Near-arrest is visible, suggesting a finite asymptotic domain size L^*, particularly in the bidisperse case. This L^* is less than a quarter of the simulation box size and not limited by finite-size effects (*11*). For the parameter values chosen (corresponding to 5-nm particles), the data shown run approximately from 6 to 300 ns in real time (*12*), with $L^* \cong 70$ nm. (At times less than 6 ns, the fluids are demixing diffusively so that sharp interfaces have not yet formed.)

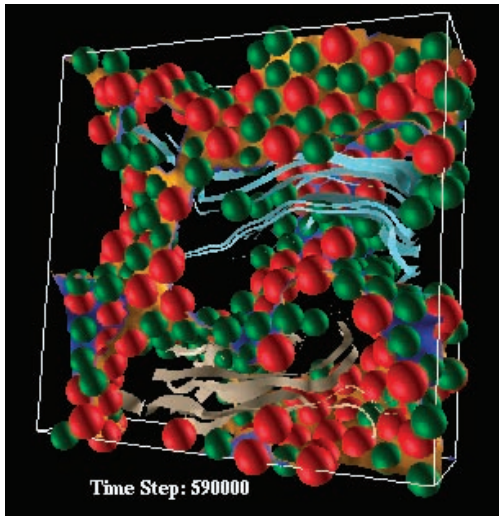

Fig. 4. A $64^2 \times 24$ section of the near-arrested bicontinuous structure in the run of Fig. 2, showing velocity streamlines for the two component fluids under cross-flow forcing with velocity $\sim 0.01\sigma/\eta$ (*12*). The group of beige-colored streamlines starting at the bottom left show flow in one fluid (the yellow side of the interface) moving rightward; the second group (blue) starting on the upper right show flow in the second fluid moving to the left. There is no discernible motion of the interfacial structure at this flow rate.

and apply even for purely repulsive particles. Any additional bonding attraction, if of sufficient strength, might enhance the rigidity of the interfacial layer, but may also cause colloidal aggregation within the bulk phase(s) before monolayer formation (*24*). Fusing the colloids after gel formation (e.g., by irradiation) would completely stabilize the structure and drastically alter the flow behavior.

Our study differs from previous work in which colloidal particles were used to stabilize spherical (*9*, *25*) and aspherical (*24*) emulsion droplets of one liquid in another. Under compression, such emulsions can form robust gel phases with interesting mechanical properties (*26*), but fluid bicontinuity is not among them. The previously preferred route to particle-stabilized emulsions involves agitation of immiscible fluids and does not appear to favor bicontinuity (*9*). Other related work (*6*, *27*–*29*) involves particles with a strong preference for one of the two liquids, creating a particle network within the chosen liquid rather than at the interface.

We expect Bijels to have several interesting physical properties beyond those discussed above. First, the fluid-bicontinuous state should remain equally insoluble on exposure to either of its solvents. This contrasts with particle-stabilized emulsion gels formed by compression (*26*), in which an excess of the continuous phase could cause droplets to separate, losing macroscopic rigidity. In Bijels this will not happen, because neither of the two interpenetrating fluids can alter its volume without also increasing the total interfacial area. The Bijel can thus metastably support simultaneous coexistence with bulk phases of both fluids. This is reminiscent of an equilibrium property of middle-phase microemulsions, which are bicontinuous states with an interface stabilized by amphiphilic molecules (*30*). In contrast to Bijels, such microemulsions are not gel phases, but inviscid fluids, as a result of their high interfacial mobility.

Second, fluid bicontinuity imparts high permeability of the gel to either of its component solvents, and any reagents dissolved in them. Accordingly, Bijels may have potential as media for continuous-process microreactions (*31*, *32*). Specifically, a static gel could support a steady permeation flow of both fluids simultaneously in opposite directions. This would bring two molecular reagents, soluble only in mutually immiscible fluids, into intimate contact at the fluid-fluid interface in the interstitial regions between the colloids. Reaction products soluble in either phase would be swept out continuously. As a test of this concept, Fig. 4 shows a simulation in which the two fluids are moving through the structure in opposite directions. On the time scale of our simulation, the gel has easily enough mechanical integrity to sustain this cross-flow without breaking up. Within the mapping onto physical parameters made previously, the chosen cross-flow fluid velocity $v = 0.01\sigma/\eta$ is ~ 10 cm s^{-1}; this is an extremely large value, given the pore scale L^* of only 70 nm. Local shear rates are $\sim 10^6$ s^{-1}.

In summary, we have presented simulation data showing formation of a self-assembled bicontinuous structure with interfacially sequestered particles. This followed a kinetic pathway involving a colloidal suspension in a binary solvent, initially miscible, that undergoes a temperature quench. Our simulations show a drastic curtailment of coarsening, consistent with eventual structural arrest: a scenario further supported by higher resolution studies of appropriate structural motifs (bumps and necks). This suggests a route to the creation of a new class of gels, Bijels, with potentially distinctive physical properties.

References and Notes

1. G. M. Whitesides, B. Grzybowski, *Science* **296**, 2418 (2002).
2. P. Poulin, H. Stark, T. C. Lubensky, D. A. Weitz, *Science* **275**, 1770 (1997).
3. W. C. K. Poon *et al.*, *Phys. Rev. Lett.* **83**, 1239 (1999).
4. A. Imhof, D. J. Pine, *Nature* **389**, 948 (1997).
5. V. J. Anderson, H. N. W. Lekkerkerker, *Nature* **416**, 811 (2002).
6. V. N. Manoharan, M. T. Elsesser, D. J. Pine, *Science* **301**, 483 (2003).
7. K. N. Pham *et al.*, *Science* **296**, 104 (2002).
8. British Patent Applications 0414829.2 and 0417437.1. (This patent refers to Bijels as "fluid-bicontinuous particle-stabilized gels.")
9. R. Aveyard, B. P. Binks, J. H. Clint, *Adv. Colloid Interface Sci.* **100–102**, 503 (2003).
10. A. J. Bray, *Adv. Phys.* **43**, 357 (1994).
11. V. M. Kendon, M. E. Cates, I. Pagonabarraga, J.-C. Desplat, P. Bladon, *J. Fluid Mech.* **440**, 147 (2001).
12. Computational methods are described as supporting material on *Science* Online.
13. K. Stratford, R. Adhikari, I. Pagonabarraga, J.-C. Desplat, *J. Stat. Phys.*, in press; preprint available at http://arxiv.org/abs/cond-mat/0407631.
14. N.-Q. Nguyen, A. J. C. Ladd, *Phys. Rev. E* **66**, 046708 (2002).
15. J.-C. Desplat, I. Pagonabarraga, P. Bladon, *Comput. Phys. Commun.* **134**, 273 (2001).
16. R. Adhikari, K. Stratford, M. E. Cates, A. J. Wagner, *Europhys. Lett.* **71**, 437 (2005).
17. A. J. C. Ladd, *J. Fluid Mech.* **271**, 285 (1994).
18. The true equilibrium state of the system investigated here consists of two bulk fluid phases separated by a single flat interface; a thermodynamically negligible fraction of the colloidal particles densely coat this interface, but the rest are spread through the fluid phases with the same uniform volume fraction as in the initial state. This minimizes interfacial area and maximizes colloid entropy.
19. M. E. Cates *et al.*, *J. Phys. Condens. Matter* **16**, S3903 (2004).
20. W. B. Russel, D. A. Saville, W. R. Schowalter, *Colloidal Dispersions* (Cambridge Univ. Press, Cambridge, 1999).
21. E. D. Siggia, *Phys. Rev. A.* **20**, 595 (1979).
22. A. Donev, S. Torquato, F. H. Stillinger, *J. Comput. Phys.* **202**, 737 (2005).
23. A. J. Liu, S. R. Nagel, *Nature* **396**, 21 (1998).
24. P. S. Clegg *et al.*, in preparation; preprint available at http://arxiv.org/abs/cond-mat/0508088.
25. A. D. Dinsmore *et al.*, *Science* **298**, 1006 (2002).
26. S. Arditty, V. Schmitt, J. Giermanska-Kahn, F. Leal-Calderon, *J. Colloid Interface Sci.* **275**, 659 (2004).
27. D. Beysens, T. Narayanan, *J. Stat. Phys.* **95**, 997 (1999).
28. G. W. Peng, F. Qiu, V. V. Ginzburg, D. Jasnow, A. C. Balazs, *Science* **288**, 1802 (2000).
29. V. J. Anderson, E. M. Terentjev, S. P. Meeker, J. Crain, W. C. K. Poon, *Eur. Phys. J. E* **4**, 11 (2001).
30. S. A. Safran, *Statistical Thermodynamics of Surfaces, Interfaces, and Membranes* (Westview, Boulder, CO, 2003).
31. There is an established technology for microreactors based on discrete droplet emulsions, but continuous operation is not possible unless all reagents and products are soluble in the continuous phase [see, e.g., (*32*)].
32. P. L. Luisi, M. Giomini, M. P. Pileni, B. H. Robinson, *Biochim. Biophys. Acta* **947**, 209 (1988).

33. We thank P. Clegg, S. Egelhaaf, E. Herzig, W. Poon, and B. Binks for discussions of their ongoing experiments on colloidal jamming at interfaces. We thank E. Weeks for advice on visualization, A. Donev for supplying code for the algorithm used to create initial conditions for the structural motif work, and C. Rutherford for discussions. This work was supported by the Engineering and Physical Sciences Research Council through grants GR/S10377 and GR/R67699 (RealityGrid). I.P. acknowledges financial support from Direccion General de Ciencia y Tecnologia of the Spanish Government and from Departament d'Universitats, Recerca i Societat de la Informacio, Generalitat de Catalunya (Spain).

Supporting Online Material

www.sciencemag.org/cgi/content/full/309/5744/2198/DC1
Materials and Methods
Figs. S1 and S2
References and Notes
Movies S1 to S3

24 June 2005; accepted 18 August 2005
10.1126/science.1116589